

Wearable Textile Antenna on Electromagnetic Band Gap (EBG) for WLAN Applications

M.S.M.Isa¹, A.N.L.Azmi¹, A.A.M.Isa¹, M.S.I.M.Zin¹, M.S.M.Saat¹, M. Abu¹, A. Ahmad²

¹Faculty of Electronic and Computer Engineering

²Faculty of Information and Communication Technology
Universiti Teknikal Malaysia Melaka (UTeM)

Melaka, Malaysia

saari@utem.edu.my

Abstract—This paper presents a new dual band wearable textile antenna for on body application, at 2.4 GHz and 5.2 GHz. The performance of the antenna is described with the integration of an electromagnetic band gap (EBG) structure. The antenna and EBG structure are made of jeans material which has a dielectric constant of 1.7, with the thickness of 1.2 mm and 0.025 loss tangent. The conductive component used in this paper is copper tape with thickness of 0.02 mm. The EBG array consists of 6 elements which are arranged in circular pattern surrounding the antenna patch. The effect of placing the EBG below the conventional antenna is studied and compared with the performance of the antenna alone. The gains of the antenna are improved by 63.7% and 121.4% at 2.4 GHz and 5.2 GHz respectively after integrating the EBG structure. At least 10 dB of backward radiation is reduced with the presence of the EBG structure. The integration of EBG with the conventional antenna has improved the antenna performance. The simulated and measured return loss, together with E-plane and H-plane polar pattern are presented in this paper for both conditions.

Index Terms—Wearable textile antenna, on body application, Electromagnetic Band Gap (EBG) structures, backward radiation, dielectric constant, loss tangent.

I. INTRODUCTION

IN recent years, there has been rapid growing of studies on wearable antenna structures for on-body [1-3]. Wearable antennas are normally been produced from various types of textile materials with different design topologies. Such antenna systems are typically introduced for motion detection especially during exercise such as monitoring heart rate and blood pressure, as well as for emergency services. Authors have reported on single frequency band wearable antenna [1, 3] and few authors also have reported on rectangular dual frequency wearable antenna. In this paper, a circular wearable antenna has been presented to study the effect of circular patch antenna incorporated with electromagnetic band gap structure (EBG) for Wireless Local Area Network (WLAN) applications.

The EBG technologies at microwave frequencies are suggested for improving the performance of the antenna

especially for the improvement of gain and reducing their sizes [4].

The main advantage of introducing EBG structure for wearable antenna design is their ability to suppress the surface wave and reducing backward radiation of the antenna for on-body applications [5]. With the generation of the surface wave, the antenna efficiency will be reduced and the radiation pattern degrades.

This paper presents a study of a dual frequency band textile wearable antenna on EBG structure for circular microstrip patch antenna design. This antenna can be worn for dual frequencies which covers 2.4 GHz and the 5.2 GHz wireless band. The circular patch antenna is matched with 50 impedance using microstrip feed line which it is easy to match, easy to fabricate and low spurious radiation from the feed line [6].

II. MICROSTRIP PATCH ANTENNA

Microstrip patch antennas have various advantages for antenna technology as it is low cost, ease of fabrication, light weight and low profile antenna [6-8]. A microstrip patch antenna has the basic geometry which consists of a metallic printed patch on a substrate which is grounded with conducting material. Some antenna shapes that are commonly used are rectangular, circular and annular-ring.

Microstrip antennas show good response for radiation modes using different feeding techniques which lead to good impedance matching between the feed line and the patch. One of the easiest feeding method to fabricate is microstrip feed line technique.

This technique can be considered as the patch extension or edge feeding which it is easy to match the antenna by controlling the inset feed. An inset cut is normally introduced at the edge of the patch to increase the performance of the impedance matching.

However, for thicker substrate, the edge feed will experience spurious radiation which will affect the bandwidth of the antenna. The spurious radiation is caused by the feed line and will improve the bandwidth of the antenna [9]. The

width of the feed line can be determined by taking the 50Ω impedance into account.

This method can be used using simulation tools or by using the equation (1) of effective dielectric constant.

$$\epsilon_{eff} = \frac{\epsilon_r + 1}{2} + \frac{\epsilon_r - 1}{2} \left[1 + 12 \frac{h}{w} \right]^{-1/2} \quad (1)$$

A. Circular Patch

A circular microstrip antenna consists of a planar resonant radiator with radius of a , which is placed in parallel with the ground plane. Both patch and ground plane are separated by a dielectric thin layer which have the relative permittivity of ϵ_r and thickness of h . Basically, the resonant frequencies of a circular patch for TM modes is given as (2) [10].

$$f_0 = \frac{c}{2\pi a \sqrt{\epsilon_r}} x'_{mn} \quad (2)$$

where ϵ_r and x'_{mn} are the relative permittivity of the substrate and the root of Bessel function respectively. For x'_{mn} , the m and n notation represents the wave number of the resonant mode of certain frequencies. In this case, the dominant mode for circular patch with radius a is x'_{11} which is 1.842. Microstrip patches commonly undergo fringing effect. The amount of fringing effect is a function of the dimension of the patch and the height of the substrate of an antenna. In order to include fringing effect in circular patch, the effective radius of the patch can be calculated using (3) [11].

$$a_e = a \sqrt{1 + \frac{2h}{\pi a \epsilon_r} \left[\ln\left(\frac{\pi a}{2h}\right) + 1.7726 \right]} \quad (3)$$

where a , h and ϵ_r represents the radius of the patch, substrate thickness, and also the relative permittivity of the dielectric substrate respectively.

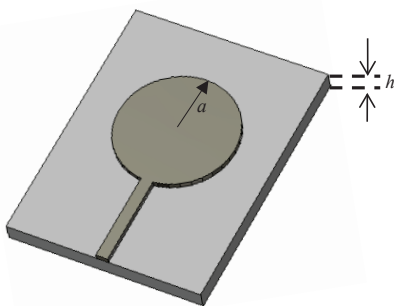


Figure 1: Conventional circular patch antenna

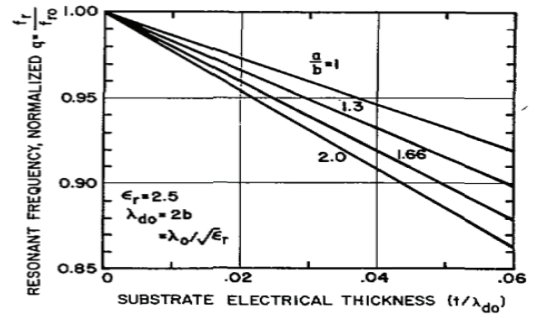


Figure 2: Dependence of normalized resonant frequency on substrate thickness [12]

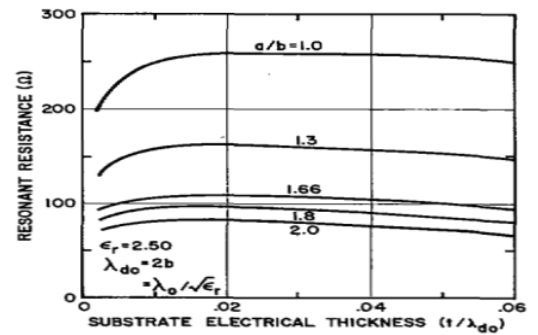


Figure 3: Dependence of resonant radiation resistance on substrate thickness for circular microstrip patch [12]

Figure 1 shows the conventional circular patch antenna. The most important parameter of designing a microstrip patch antenna is the need of selecting a better substrate material constant tolerance control. The resonance frequency of the antenna depends on the substrate thickness and radius of the patch in which the behavior between the parameters is shown in Figure 2 for dielectric constant of 2.5. The calculation of wall admittance of a circular patch is complex as stated in [13]. Therefore, more accurate calculations can be made if the values of the wall susceptance are made available accurately [12].

The curve shown in Figure 2 is based on the validation of the wall admittance which is shown in [13]. In addition, Figure 3 presents the relation between the substrate thicknesses to the resonant resistance of the patch. The resonant resistance increases with the increment of both patch radius and substrate thickness. The accuracy of the curve shown in Figure 3 is also based on the wall conductance given by [13]. It is important to know the effect of the substrate thickness on the resonant frequency and the resonant resistance due to the accuracy of the wall conductance as it affects the conductivity of the patch antenna.

III. ELECTROMAGNETIC BAND GAP

Periodic electromagnetic band gap (EBG) materials have been recently used with the purpose of modifying the radiation pattern [14-16] of an antenna and overall arrays characteristics[17, 18] including scan blindness for phased array antenna[19]. EBG structures are usually being formed in a periodic arrangement of dielectric materials and also metallic conductors. There are three groups of EBG categories accordingly to the EBG's geometric configurations which are three-dimensional volumetric structures, two-dimensional planar surfaces, and one-dimensional transmission lines. The most widely used EBG group is the two-dimensional planar surfaces such as mushroom-like EBG surface. Mushroom-like surface is called by its name because of the presence of the pin via at the center of the EBG as shown in Figure 4.

In early research, there are difficulties to minimize the size of the EBG structures. It is inconvenient for an EBG structure to have a small physical size since the period of the EBG should be at least half-wavelength at the stop band frequency. Therefore, mushroom-like structure is one of the best techniques to improve the compactness of the EBG design [4]. The mechanism of the operation of an EBG structure can be explained by the LC network distribution. For mushroom-like EBG structure, the equivalent LC circuit is considered as a two-dimensional electrical filter for the blockage of surface wave. Current flowing through the pin via produces the inductance, L while the capacitance, C results from the gap between the patches.

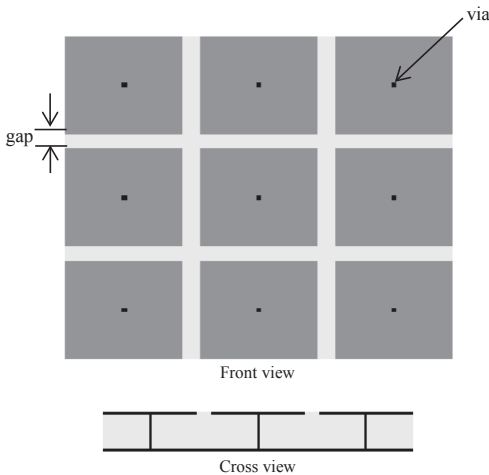


Figure 4(a): Mushroom-like EBG Surface

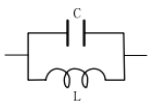


Figure 4(b): Equivalent LC circuit

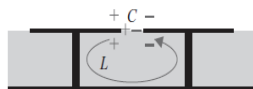


Figure 4(c): LC model

Figure 4: Mushroom-like EBG geometry [20]

Referring to the equation of center frequency as in (4), increasing the inductance or capacitance will affect the decrease in the band-gap position of the EBG which will reduce the size of the structure [5].

$$f_c = \frac{1}{2\pi\sqrt{LC}} \tag{4}$$

The fringing capacitance between adjacent coplanar metallic plates gives the value of the capacitor, C. The derivation of the edge capacitance for a narrow gap EBG structure is given as (5).

$$C = \frac{W\epsilon_0(1+\epsilon_r)}{\pi} \cosh^{-1} \left(\frac{W+g}{g} \right) \tag{5}$$

where W, ϵ_r and g are the width of one unit cell EBG, permittivity of dielectric substrate and the gap between elements, respectively.

Figure 4(c) shows the LC model of an EBG structure which the current loop derives the value of the inductor. The inductance of an EBG circuit depends on the thickness and the permeability of the structure itself.

$$L = \mu h \tag{6}$$

By substituting both equation (5) and (6), the computation of surface impedance and resonant frequency can be made [20].

IV. ANTENNA WITHOUT EBG

In this section, the wearable textile antenna is analyzed in free space without the integration with EBG structure. The antenna structure designed for this research purpose is to cover frequency bands of 2.4 GHz and 5.2 GHz which is applicable for wireless networking bands.

A. Antenna Design

The proposed antenna in this paper is chosen based on a design for textile antenna for wearable body area application [21]. The antenna design is printed on a 70x90mm² jeans substrate material with relative dielectric constant of 1.7 and thickness of 1.2mm. The selection of the material is based on its high tensile strength, very good electric property, and high durability as stated in [21]. The conducting components such as the coplanar feed line, radiating elements, and ground plane are made of copper tape which has the thickness of 0.02mm. Commercial electromagnetic simulation software, CST Microwave Studio is used during the design process.

In order to design the conventional antenna, the calculation is done using equation (1) until (3). Some optimization is needed to make sure that the antenna operates well at both operating frequencies. The optimized geometry of the proposed design is illustrated in Figure 5 and the dimensions of the design are listed in Table 1. A circular disc antenna is designed with a radius of 22mm and a circular slot inside it in order to perform dual band antenna.

Table 1
Dimension of Proposed Circular Patch Antenna

Parameters	Dimensions (mm)	
	Conventional	Optimized
Width of Substrate (W_s)	121.83	70
Width of Ground (W_g)	77.8	70
Width of Microstrip Feed I (W_{f1})	4.3	4.3
Width of Microstrip Feed II (W_{f2})	-	2
Width of Inset Feed (W_{inset})	-	1
Length of Substrate (L_s)	121.63	90
Length of Ground (L_g)	77.8	30
Length of Microstrip Feed I (L_{f1})	-	8
Length of Microstrip Feed II (L_{f2})	-	23
Length of Inset Feed (L_{inset})	-	5
Radius of Slotted Circular	$R_1 = 13$	$R_1 = 8$
Radius of Circular Disc	$R_2 = 28.1$	$R_2 = 22$
Gap between slot (g)	-	1
Thickness of Substrate (h)	1.2	1.2
Thickness of Patch	0.02	0.02
Thickness of Partial Ground Plane	0.02	0.02

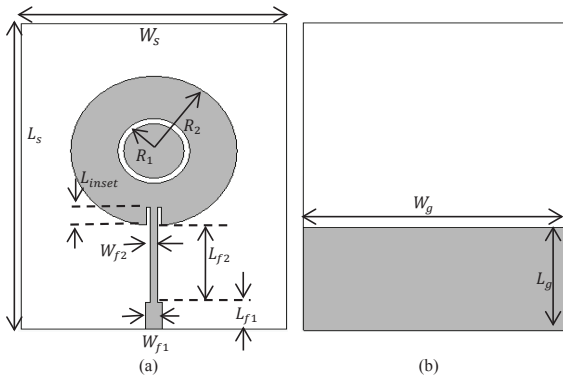


Figure 5: Geometry of circular monopole patch antenna
(a) Front view (b) Back view

B. Simulation and Measurement Result

The antenna performances such as the return loss, impedance matching, antenna efficiency, and radiation pattern are evaluated for the operating frequencies at 2.4 GHz and 5.2 GHz. The simulated and measured reflection coefficient (S_{11}) of the antenna is represented in Figure 6. The proposed antenna resonates at 2.4 GHz and 5.2 GHz for WLAN applications with performances as listed in Table 2. The simulation result shows that there is only 2.3% signal loss at low resonant frequency and 0.02% signal loss at high resonant frequency. The percentage of signal loss measured for this antenna is 5.4% and 1.6% at 2.4 GHz and 5.2 GHz.

The results show good agreement between simulation and measurement of the antenna. However, there are some difference between the result of simulation and measurement. Lower return loss is found from the measurement result which caused by the cable loss during the measurement process. The fabricated structure is prepared manually, hence affecting the performance of the antenna. The fabricated structure of the antenna can be referred at Figure 11. The results of the

antenna operating at both frequency show that the antenna performs good characteristics which have a very high efficiency percentage. In the design, the circular ring affects the operating frequencies of the structure where the outer ring acts as a radiator which resonates for low frequency while the inner ring affects radiation at high frequency. The advantage of this conventional antenna is that it also can cover ultra-wide band frequencies.

Figure 7 represented the 3D radiation pattern from the simulation of the proposed antenna. The radiation pattern of the antenna at both frequencies are expected to be likely as the fundamental of coplanar patch antenna which having radiation at both direction, forward and backward radiation. The comparison of radiation pattern can be easily made by referring at the E-plane and H-plane. The comparison between simulated and measured radiation patterns for the antenna will be discussed in the next section, together with the antenna with EBG structure.

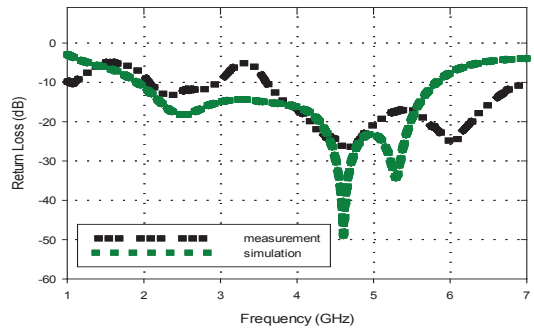
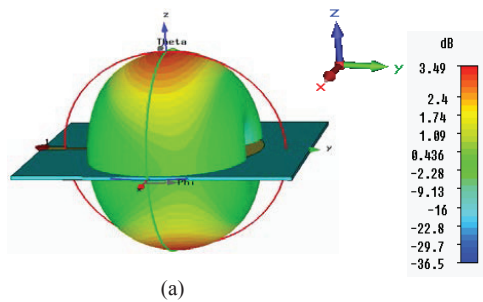


Figure 6: Reflection Coefficient of simulated and measured antenna

Table 2
Simulated Gain and Directivity for Conventional Antenna

Conventional Antenna		
Frequency (GHz)	2.4	5.2
Simulated Return Loss (dB)	-16.374	-36.362
Measured Return Loss (dB)	-12.69	-17.83
Directivity (dBi)	3.597	3.405
Realized Gain (dB)	3.488	3.376
Radiation Efficiency (dB)	-0.0073	-0.0282
Percentage Efficiency (%)	99.8	99.4



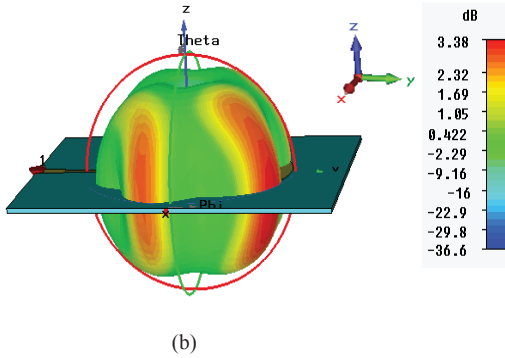


Figure 7: 3-D Radiation Pattern of Conventional Antenna
(a) 2.4 GHz (b) 5.2 GHz

V. ANTENNA WITH EBG

In this section, a wearable textile antenna integrated with Electromagnetic Band Gap (EBG) structure will be discussed. The design covers dual band WLAN frequencies, 2.4 GHz and 5.2 GHz.

A. Dual Band EBG Unit Cell

A double circular patch was designed by introducing ring to the design in order to cover dual frequency bands as shown in Figure 8. The EBG structure was optimized using the same jeans material as the textile substrate. Parameters p , r_{e1} , r_{e2} and g were obtained by optimizing the size of the conventional patch antenna. From the optimization, the period, p of the structure is found to be 49mm.

Via is placed at the center of the patch in order to block surface wave excitation within the structure. The EBG geometry determines the corresponding transmission band at 0° reflection phase. The size of outer ring of the design affects the resonance frequency of the structure. Larger patch size results a lower frequency band. Figure 9 shows the simulated S_{12} of the EBG design. By considering reflection phase from -90 to 90 degrees, the EBG are predicted to be in phase at 2.4 GHz and 5.18 GHz. Therefore, it shows that the EBG design is suitable for dual band WLAN applications. The unit cell is then duplicated to form a new structure to be integrated with the designed antenna previously.

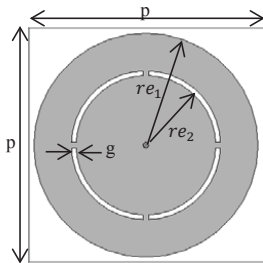


Figure 8: EBG geometry. Optimized dimension: $p=49$ mm, $r_{e1}=23.6$ mm, $r_{e2}=15.8$ mm, $r_{via}=0.6$, $g=1$

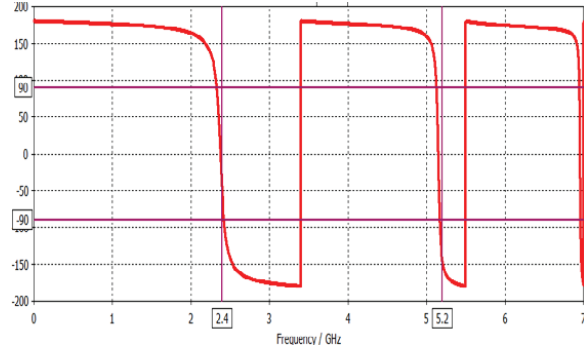


Figure 9: Reflection phase of a unit cell EBG structure

B. Antenna with EBG

The EBG design is duplicated in circular arrangement using 6 identical elements. The overall size of the structure is 172×172 mm. It is important to test the transmission response of the electromagnetic waves. Therefore, a strip line is placed on the structure to replace the antenna transmission, by connecting the strip to the ground of the EBG. The dual band antenna was next combined with the EBG structure by placing the antenna 0.5 mm away from the surface of the structure. The antenna is placed in the middle of the EBG structure.

The arrangement of the EBG elements influence some ripple to the reflection coefficient of the overall design [22]. A smoother pattern of reflection coefficient can be obtained by arranging the elements further from the antenna structure. However, it may result in increment size of the structure. Therefore, the design illustrated in Figure 10 is the best arrangement to achieve dual frequency band for wearable application purpose. The size of the outer patch in this design is the best geometry for the transmission at 2.4 GHz while the size of the inner patch gives best result at 5.2 GHz. Figure 11 shows the fabricated antenna and antenna on EBG structure.

Figure 12 illustrated the difference in reflection coefficient magnitude between the conventional antenna and the antenna integrated with EBG. Table 3 indicates the performance of antenna with EBG structure integrated below it. The gain and directivity of the design has been improved compared to the conventional antenna. By referring to the realized gain results, the gain improved by 63.7% and 121.4% at 2.4 GHz and 5.2 GHz respectively. The performance of the antenna without EBG structure has been discussed earlier in Table 2.

This design indicates that the EBG structure acts as a high impedance surface, which may reduce the backward radiation of the antenna. The reduction of backward radiation of the antenna can be seen clearly from the 3-dimension radiation pattern as shown in Figure 13. The polar patterns are measured and illustrated for both configurations; antenna with and without EBG structure as in Figure 14. The radiation pattern from measurement and simulation of conventional antenna as discussed in Section I is compared with the antenna integrated with EBG.

The radiation pattern of the conventional antenna have both forward and reverse radiation direction in the E-plane and H-plane at 2.4 GHz and 5.2 GHz. At both frequencies, the antenna has a dipole-like radiation plane in the E-plane while it is omnidirectional-like in the H-plane. The backward radiation is then being reduced at least 10 dB by integrating the EBG structure which behaves as the high impedance surface and suppress the surface current within the structure. A better improvement is identified in the E-plane configuration compared to the other plane. Other than backward radiation reduction, placing the EBG below the antenna enhanced the gain of the antenna at least 3 dB in forward direction. This demonstrates that the EBG structure improved the antenna performances. Both measurement and simulation are tolerance which proves that the antenna design is suitable for the wearable application with a low backward radiation.

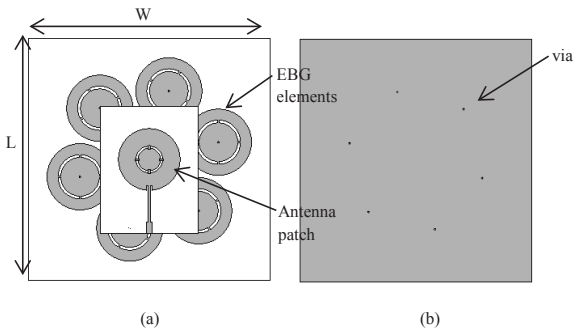


Figure 10: Geometry of circular patch antenna on EBG structure
(a) Front view: W= 172 mm, L=172 mm (b) Back View

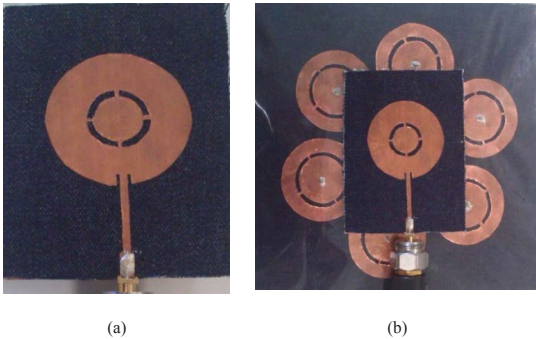


Figure 11: Fabricated wearable textile antenna
(a) Conventional antenna (b) Antenna with EBG structure

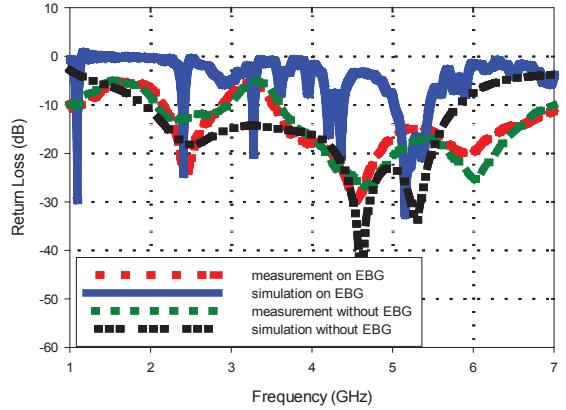
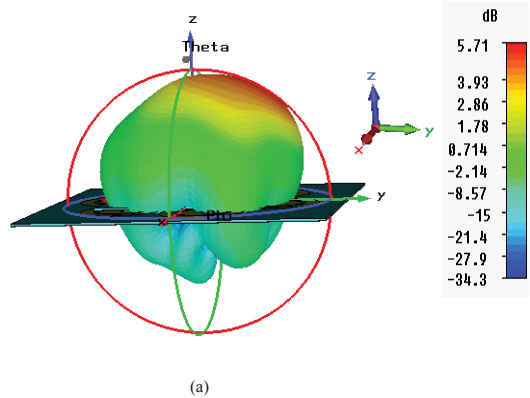


Figure 12: Reflection Coefficient of simulated and measured conventional antenna on EBG structure

Table 3
Simulated Gain and Directivity for Antenna with EBG

Antenna on EBG		
Frequency (GHz)	2.4	5.2
Simulated Return Loss (dB)	-17.85	-22.74
Measured Return Loss (dB)	-23.17	-15.15
Directivity (dBi)	8.332	7.534
Realized Gain (dB)	5.711	7.475
Radiation Efficiency (dB)	-2.5450	-0.0361
Percentage Efficiency (%)	55.7	99.2



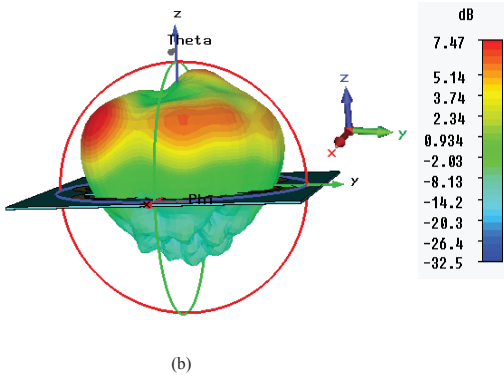
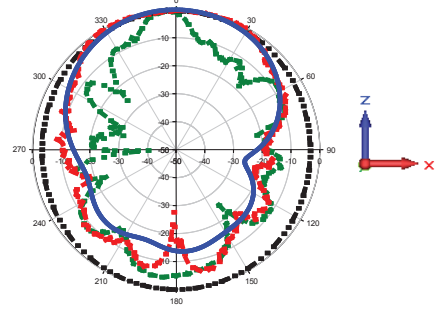
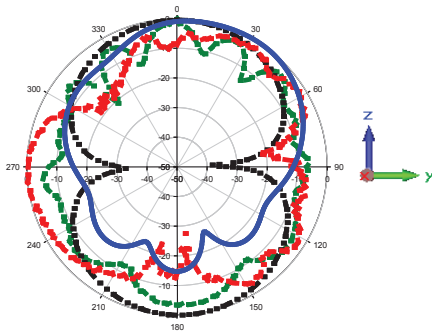


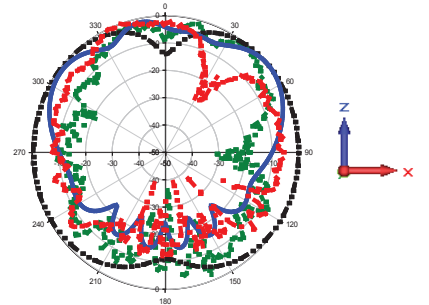
Figure 13: 3-D Radiation Pattern of Antenna with EBG (a) 2.4 GHz (b) 5.2 GHz



(c)



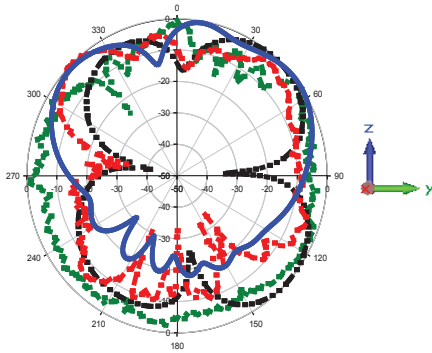
(a)



(d)

--- measurement on EBG
— simulation on EBG
--- measurement without EBG
--- simulation without EBG

Figure 14: Comparison of Simulated and Measured Radiation Pattern of Antenna with and without EBG (a) E-plane at 2.4 GHz (b) E-plane at 5.2 GHz (c) H-plane at 2.4 GHz (d) H-plane at 5.2 GHz



(b)

VI. CONCLUSION

This paper has demonstrated a wearable textile antenna with electromagnetic band gap structure which covers dual band WLAN frequencies; 2.4 GHz and 5.2 GHz. The antenna and EBG substrate are designed using jeans material with relative permittivity of 1.7. The EBG are arranged in circular pattern by duplicating 6 same elements, surrounding the patch antenna. The main problem of a wearable antenna is the backward radiation which might not be proper to be used on body. Therefore, the EBG structure is designed to reduce the backward radiation of the antenna. In this paper, the EBG structure has relatively decrease the backward radiation of the antenna in both E-plane and H-plane by at least 10 dB at the corresponding frequencies. The antenna with EBG also experiences an increment of gain with 63.7% and 121.4% increment at 2.4 GHz and 5.2 GHz respectively. Measurement of the structures also shows corresponding result with the simulation result. Overall, the design demonstrated that it is possible to produce a wearable antenna to be placed on body with as minimum spurious backward radiation as possible.

ACKNOWLEDGMENT

The authors would like to thank University of Sheffield for their facilities. Great gratitude to Universiti Teknikal Malaysia Melaka (UTeM) and Ministry of Higher Education for their “Research Acculturation Grant: RAGS/2012/FKEKK/TK02/2 B0005”.

REFERENCES

[1] J. H. Lim and H. M. Lee, "Low Specific Absorption Rate Wearable Antenna for WLAN Band Applications," *Proceedings of the Fourth European Conference on Antennas and Propagation (EuCAP), 2010*, pp. 1-5, 2010.

[2] R. Langley and S. Zhu, "Dual-Band Wearable Textile Antenna on an EBG Substrate," *IEEE Transactions on Antennas and Propagation*, vol. 57, pp. 926-935, 2009.

[3] Y. Rahmat-Samii, "Wearable and Implantable Antennas in Body-Centric Communications," *The Second European Conference on Antennas and Propagation, EuCAP 2007*, pp. 1-5, 2007.

[4] W. Wang, X.-y. Cao, R. Wang, and J.-j. Ma, "A Small Dual-Band EBG Structure for Microwave," *International Conference on Microwave and Millimeter Wave Technology, ICMMT 2008*, pp. 1637-1639, 2008.

[5] O. Ayop, M. K. A. Rahim, and T. Masri, "Dual Band Electromagnetic Band Gap (EBG) Structure," *Asia Pacific Conference on Applied Electromagnetics, 2007 (APACE 2007)*, pp. 1-3, 2007.

[6] A. Mandal, A. Ghosal, and A. Majumdar, "Analysis of Feeding Techniques of Rectangular Microstrip Antenna," *IEEE International Conference on Signal Processing, Communication and Computing (ICSPCC) 2012*, pp. 26-31, 2012.

[7] K. F. Lee and K. F. Tong, "Microstrip Patch Antennas: Basic Characteristics and Some Recent Advances," *Proceedings of the IEEE*, vol. 100, pp. 2169-2180, 2012.

[8] M. Abu, E. E. Hussin, M. S. M. Isa, Z. A. Baharudin, and Z. Zakaria, "Designing Halfring Artificial Magnetic Conductor for RFID Application," *2013 IEEE International RF and Microwave Conference (RFM)*, pp. 121-124, 2013.

[9] B. Jamali and T. Cook, "Comparative Study of Microstrip Patch Antenna Feed Network," *2013 International Conference on Radar (Radar)*, pp. 179-183, 2013.

[10] F. Abboud, J. P. Damiano, and A. Papiernik, "New Determination of Resonant Frequency of Circular Disc Microstrip Antenna: Application to Thick Substrate," *Electronics Letters*, vol. 24, pp. 1104-1106, 1988.

[11] M. S. Arifianto, Maryadi, and A. Munir, "Dual-band Circular Patch Antenna Incorporated with Split Ring Resonators Metamaterials," *10th International Conference on Electrical Engineering/Electronics, Computer, Telecommunications and Information Technology (ECTI-CON), 2013*, pp. 1-4, 2013.

[12] K. R. Carver, "Microstrip Antenna Technology," *IEEE Transactions on Antennas and Propagation*, vol. 29, pp. 2-24, 1981.

[13] K. R. Carver, "Practical Analytical Techniques for the Microstrip Patch Antenna," *Proceedings Workshop Printed Circuit Antenna Technology*, pp. 7/1-20, 1979.

[14] M. S. Mohamad Isa, R. J. Langley, and S. Khamas, "Antenna pattern diversity using EBG," *Loughborough Antennas and Propagation Conference (LAPC), 2010*, pp. 325-328, 2010.

[15] M. S. Mohamad Isa, R. J. Langley, and S. Khamas, "Antenna control using EBG," *Proceedings of the 5th European Conference on Antennas and Propagation (EuCAP)*, pp. 216-219, 2011.

[16] M. S. Mohamad Isa, R. J. Langley, S. Khamas, A. Awang Md Isa, M. S. I. M. Zin, F. M. Johar, and Z. Zakaria, "Antenna Beam Steering using Sectorized Square EBG," *Journal of Telecommunication, Electronic and Computer Engineering (JTEC)*, vol. 4, pp. 39-44, 2012.

[17] M. S. Mohamad Isa, R. J. Langley, S. Khamas, A. Awang Md Isa, M. S. I. M. Zin, Z. Zakaria, N. Z. Haron, and A. Ahmad, "A Novel Technique of Controlling Signal Propagation within Array Elements using Switchable Miniaturized Electromagnetic Band Gap," *2013 IEEE Symposium on Wireless Technology & Applications (ISWTA)*, pp. 178-182, 2013.

[18] M. S. M. Isa, R. J. Langley, S. Khamas, A. A. M. Isa, M. Zin, Z. Zakaria, N. Z. Haron, and A. Ahmad, "A Low Profile Switchable Pattern Directivity Antenna using Circular Sectorized EBG," *Journal of Telecommunication, Electronic and Computer Engineering*, vol. 5, pp. 11-18, 2013.

[19] M. S. M. Isa, R. J. Langley, S. Khamas, A. A. M. Isa, M. Zin, Z. Zakaria, N. Z. Haron, and A. Ahmad, "A Technique of Scan Blindness Elimination for Planar Phased Array Antenna using Miniaturized EBG," *Jurnal Teknologi*, vol. 69, 2014.

[20] F. Yang and Y. R. Samii, *Electromagnetic Band Gap Structures in Antenna Engineering*. United Kingdom: Cambridge University Press, 2009.

[21] S. D. Md. Shaad Mahmud, "Design and Performance Analysis of a Compact and Conformal Super Wide Band Textile Antenna for Wearable Body Area Applications," *EuCAP*, pp. 1-5, 2012.

[22] M. S. Mohamad Isa, R. J. Langley, S. Khamas, A. Awang Md Isa, M. S. I. M. Zin, F. M. Johar, and Z. Zakaria, "Microstrip Patch Antenna Array Mutual Coupling Reduction using Capacitive Loaded Miniaturized EBG," *Journal of Telecommunication, Electronic and Computer Engineering (JTEC)*, vol. 4, pp. 27-34, 2012.